Proceedings of the 8th U.S. National Conference on Earthquake Engineering
April 18-22, 2006, San Francisco, California, USA
Paper No. 1587

EARTHQUAKE DEFORMATION ANALYSIS USING TERRESTRIAL SCANNING LASER -LIDAR TECHNOLOGY

Robert KAYEN[1], Brian D. COLLINS[1], Gerald BAWDEN[2], Robert T. PACK[3]

ABSTRACT

Earthquakes leave in their wake permanently deformed ground. These deformations take on extremely complex surfaces and shapes. A new technology, 3-D laser-scanning Light Detection And Ranging (LIDAR), allows for the rapid and remote sensing of damaged terrain to construct ultra-high resolution 3-D models of the ground. Scanning LIDAR targets the damaged area with sequenced LASER pulses that, in aggregate, provide the basis for a digital terrain model of the damaged region. Terrestrial LIDAR surveys, using a tripod mounted ground-based laser scanner, are the optimal tool for post-disaster characterization of deformations. Ground–based LIDAR has an accuracy range of 0.3-1.5 cm and a sub-centimeter target-area footprint, with a data collection range distance up to 1500 meters. LIDAR deployments rapidly gather millions of target point locations, their natural color, and their laser pulse attenuation characteristics. These data are then available for visualization and analysis of the permanent ground deformations, and establishment of ultra-high precision baseline surveys for change detection. In this paper, we present examples of geometric measurement and change detection in LIDAR studies of fault displacement, soil liquefaction-induced lateral spreading, and seismically-induced landslides from the 2004 Parkfield, California and 2004 Niigata Ken Chuetsu, Japan, Earthquakes. High resolution images and movies of these LIDAR data can be viewed at http://walrus.wr.usgs.gov/geotech/LIDAR.html.

Introduction

LIDAR (LIght Detection And Ranging) has proven useful in engineering geologic applications (Pack, 2002) and for the monitoring of ground movements (Kayen et al, 2004; Bawden et al. 2004). LIDAR systems have been applied to landslides in Europe (Paar et al, 2000; Scheikl et al., 2000; Rowlands et al. 2003; Lim et al. 2005), in the U.S. (Collins and Sitar, 2004, 2005), and in Japan (Kayen et al., in press). In this paper the focus of LIDAR application is on deformed ground and damaged structures caused by earthquakes. This paper assesses the ability of the technology to (1) image ground and structural deformations; (2) develop and archive example three-dimensional imagery of surface deformation caused by landslides and liquefaction; and (3) establish an ultra-high precision baseline survey for future change detection.

LIDAR technology is a natural extension of laser range finder systems or electronic distance meters (EDMs) used commonly in survey applications. With this technology, a laser beam is pulsed along a known and constantly changing trajectory to acquire the precise distance to objects across a given area. Each pulse reflects from the object back to the scanner. By

timing the round trip of each laser pulse, the range is determined directly and a series of spherical coordinates are recorded. Knowing the position and orientation of the instrument, a group of x,y,z coordinates (referred to as a "point cloud") is acquired at a very rapid rate. As the laser pulses reflect from objects at various distances from the scanner, point measurements are collected that define the object's shape. In addition, modern LIDAR systems have onboard CCD cameras to record the natural color of the objects as well as the intensity of returned laser light providing additional object data.

Data Acquisition Using Terrestrial LIDAR Technology

Three different terrestrial LIDAR systems are used by the authors, each with its own advantages. The USGS Coastal and Marine Geology system and USU systems (author affiliations 1 and 3) are based on the same near-infrared rotating LIDAR transceiver manufactured by Riegl (www.rieglusa.com). The third system, used by the USGS Water Resources Division (author affiliation 2) is a fixed-base Optech ILRIS-3D unit (www.optech.ca/). All three systems are portable and are designed for the rapid acquisition of high-resolution three-dimensional imagery under outdoor conditions. The maximum distance to targets these lasers can sense is between 700m and 1500m under the best atmospheric conditions, though typically they have a working range of 500m. The minimum target distance is between 2-3 m. The accuracy of the Riegl systems is consistently about 1.5 cm at most ranges, whereas the Optech unit has higher accuracy of about 0.3 cm, owing to the type of laser used (Riegl's laser diode verses Optech's solid state laser).

The two Riegl-based systems of the USGS and USU employ different scanning methods. The USGS system uses a cylindrical Riegl Z210 scanner (Figure 1a). With this system, a single scan can sweep up to 336° horizontally and 80° vertically. The scanner makes millions of individual x, y, z position measurements, at a rate of 8,400 points/second. Thus, the time required for scanning the highest density of points per setup (5.6 million targeted points) is 11 minutes. Point measurements at a coarser density, from hundreds of thousands to two million target points, takes less than several minutes. The USU Riegl Z210 system uses a pan and tilt scanner head that is eight times slower than the USGS system such that some scans can take over an hour to complete. The second USGS system, the Optech ILRIS scans at a rate of 2,000 points/second. Thus, the same 5.6M point acquisition would take about 47 minutes. The Optech system has a fixed base and acquires data within a 40°-by–40° window per individual scan (Figure 1b), and the scanner head must be moved to expand the scan area. The advantage of the fixed base Optech system is that it produces a scan of higher accuracy, and it is the optimal unit when millimeter-scale precision is needed. The manufacturer now provides a rotating base for the unit to collect multiple windows from the same unit.

The time required for set up of the LIDAR systems can exceed the scan time. Optimizing the transportation and set up of these units is critical for efficient scanning. The typical set up for the LIDAR system is on a tripod set on the ground (Figure 1a, 1b, 2a). However, we have found that permanently bolt-mounting the scanner tripod to the roof of a vehicle, and rapidly moving between fixed scan locations with the data acquisition system running allows for the most time-efficient method of collecting data (Figure 1c). This method has the added benefit of elevating the scanner to about 3 meters above the ground, optimizing

data coverage and moving the scanner into the manufacturer recommended minimum distance from the ground immediately around the tripod. We have found that about 60-80 roof-mounted surveys can be performed on a typical survey day using the Riegl unit, as compared with 10-15 ground tripod surveys.

The LIDAR systems have the ability to collect color information about each target point. The USU system includes a custom developed Texel Camera™ that collects 100 pixels of high-

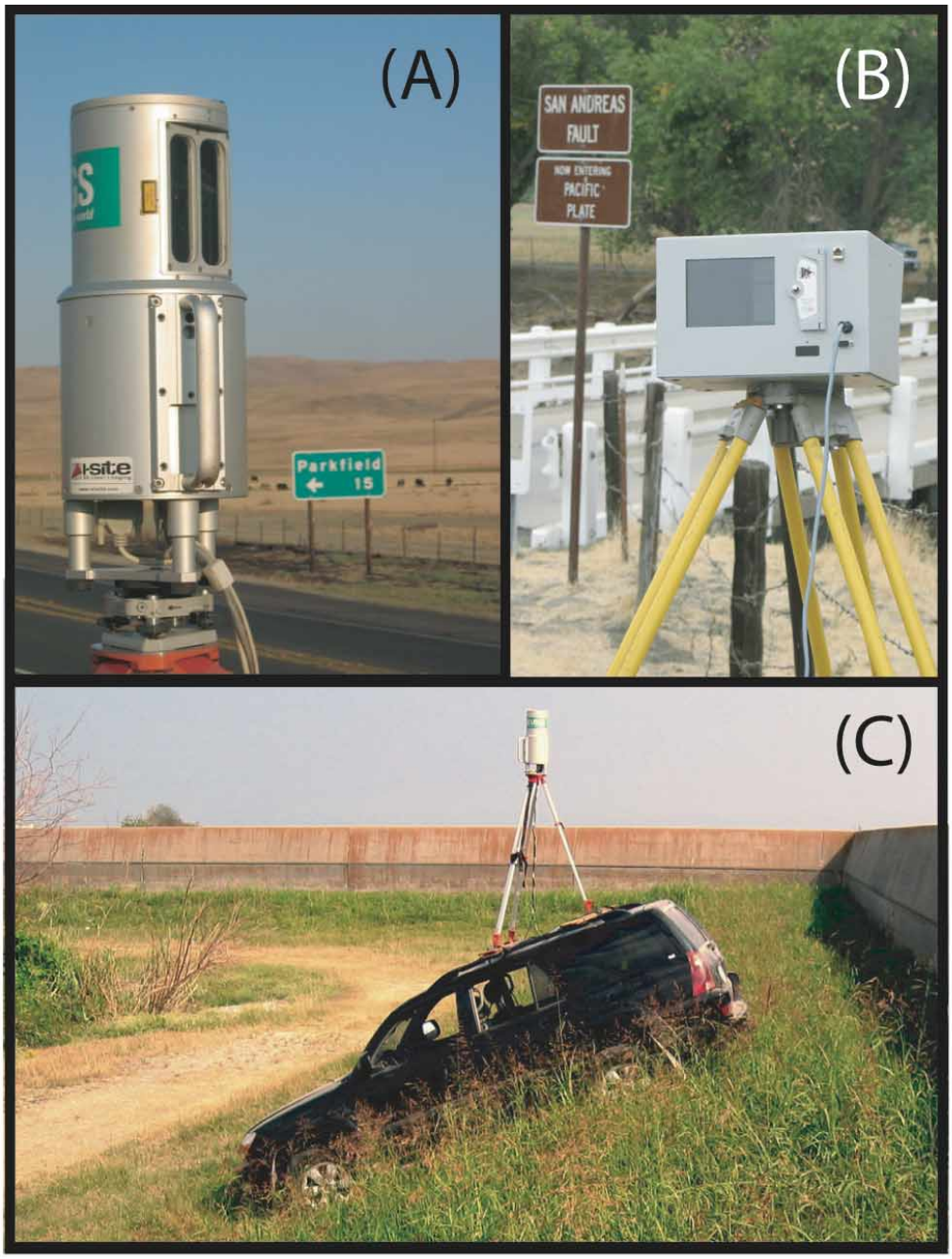

Figure 1. (a) The Riegl Z210 unit measuring fault after-slip in Cholame and (b) the Optech ILRIS unit at the Parkfield Bridge, both following the 2004 Parkfield Earthquake; (c) Roof mounted LIDAR scanning of over-topped New Orleans levees following the 2005 Hurricane Katrina.

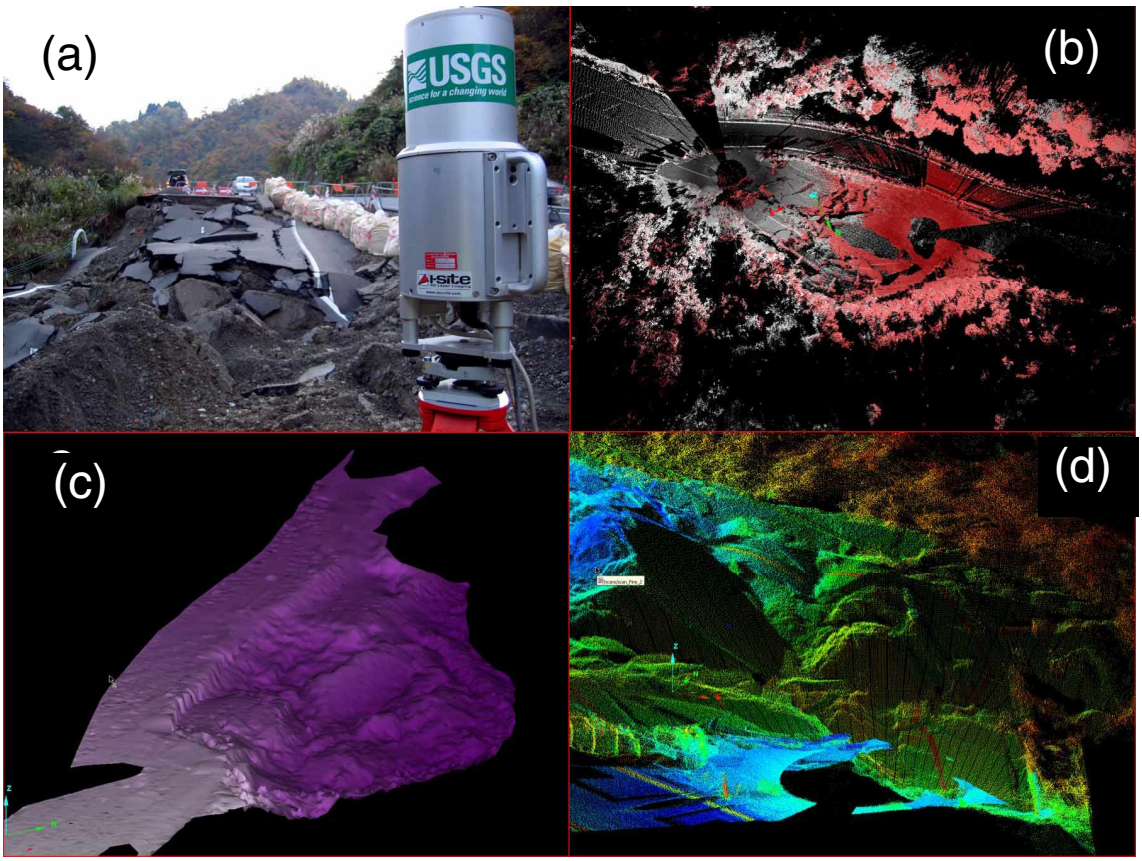

Figure 2. Processing procedures for ground-LIDAR technology: (a) scanning target; (b) Merging multiple scans to minimize shadow zones; (c) Rendering a solid surface model; (d) High precision measurement and change detection of ground and structural deformations.

resolution color data within the area of each laser footprint. This provides an improved ability to automatically drape a detailed color "texture" onto a three-dimensional (3-D) surface model (Figure 3). In comparison, the USGS Riegl system records a single pixel of color for each laser point in the point cloud. The result is a lower resolution color texture than collected with the USU system.

Several useful applications of the color and laser intensity channels include the extraction of non-topographic textural information about the target, identification of color-based lithologic changes, and enhancement and identification of geo-referencing reflectors that send back strong reflected signals (Kayen et al., 2004).

The 3-D laser scanners cannot see behind objects, and so the first surface encountered casts a shadow over objects behind it. For example, in a scan of an road embankment failure of the 2004 Niigata-Chuetsu earthquake (Figure 2b), the near-field objects cast shadows over the debris located behind them. As the incident angle of the laser point decreases, proportionally

larger shadows are cast on the ground behind the target. To minimize shadow zones and get full coverage of the target surface, the scanner is moved to other locations surrounding the target zone. Multiple setups limit the number of shadow zones while also increasing the resolution of the target shape and the outermost boundaries of the scanned area.

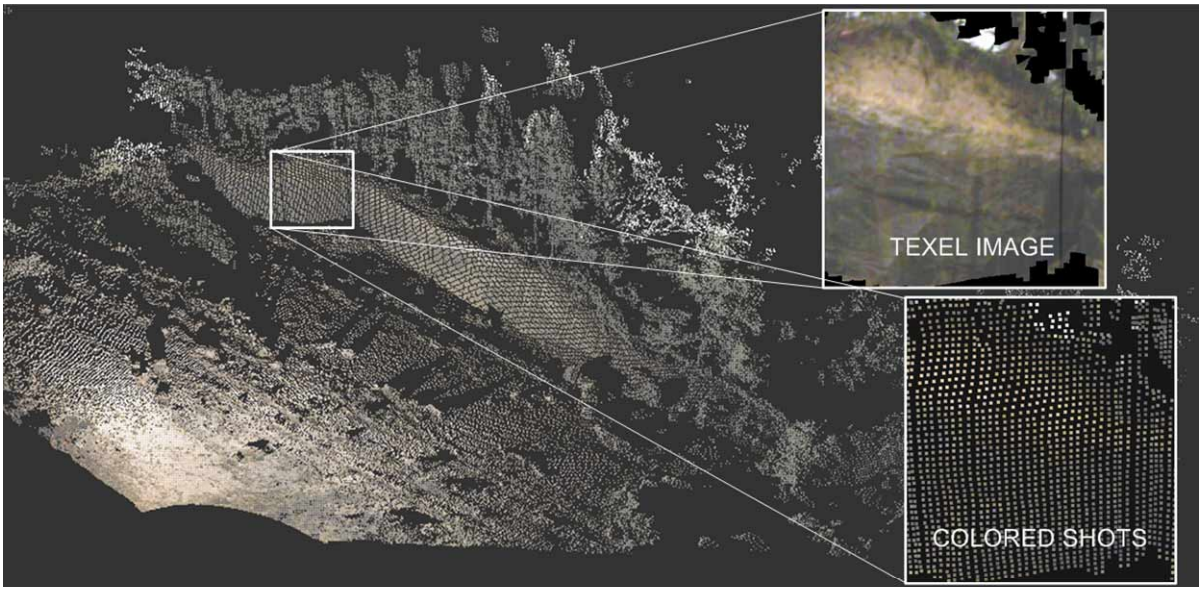

Figure 3. Color 3D image of a rockslide near Ojiya, Japan with a close-in views of the side-scarp. The two thumbnail images illustrate the enhanced quality of the Texel image when compared to the colored LIDAR point cloud.

Data Processing Of Terrestrial LIDAR Measurements

Manipulation of a typical scan data set containing many millions of data points requires computers with high processing speeds, large capacity dynamic RAM memory, a large dedicated graphics memory buffer, and specialized surface modeling software. The USGS systems utilize two surface modeling software packages, I-SiTE Studio (I-Site, 2005) and PolyWorks (Innovmetric, 2005). The USU system uses custom USU LIDAR control software and LDViewer™ and LD Modeler™ software by Rappid Mapper Inc. (RMI, 2004). These software packages collect the scan point-cloud data and can process multiple scans into a single geo-referenced data set. The four frames of Figure 2 show the processing steps needed for producing a surface model and computing deformations: (a) scan the target from multiple perspectives; (b) merge and register the scans; (c) filter out vegetation and render the surface model; and (d) compute and analyze deformations.

Data registration typically consists of georeferencing multiple scans to each other using either a local or global coordinate system. A least squares "best-fit" match is made between scans, and can be augmented by precise survey measurements. Filters are then used to eliminate unwanted data. For example, filters can be used to remove vegetation so as to observe the bare earth. The filtered point-data can then be "segmented" to differentiate discrete surfaces from each other and from complex objects like trees and brush. Surfaces are produced by creating triangular irregular networks (TIN) of the point cloud data. The TIN can be used as working digital terrain

model (DTM) representing ground topography or as surface form of a structure. The surface model can be used to document the condition of the ground or structure and provides a baseline for change detection of volumes, areas, and distances.

Geometric Analysis Using LIDAR Data

The primary measurements that can be made on ground and structures damaged by earthquakes using a LIDAR DTM surface are distance, surface area, volume, rotation, and settlement. An example of recent earthquake-induced structural damage that has been analyzed by LIDAR is presented in Figure 4, which shows the damaged portal of the Juetsu railroad tunnel, following distress during the 2004 Niigata-Chuetsu earthquake (Kayen et al., in press). The portal is founded on a poorly compacted embankment fill that settled during the earthquake. The portal pulled away from the tunnel, opening a gap, and slid downslope toward the right in Figure 4a. Vertical settlement was more pronounced on one side of the portal causing it to undergo a minor rotation. In the interior of the tunnel, displacement of the portal was observed in the walls and ceiling, out of reach of the reconnaissance team members. An oblique view of the LIDAR point-cloud data can be seen in Figure 4b. Here, the portal (front section) and tunnel are viewed from above and south of the portal entrance. The left-lateral offset of the portal relative to the tunnel is clearly visible in the LIDAR model. In the LIDAR imagery, precise centimeter-scale measurements can be made of the three-dimensional deformation of the structure. At this tunnel, 36 cm of separation of the portal and 21 cm of left-lateral displacement, visible in 4c was measured in the LIDAR imagery. Displacement of the portal and failure of the gravel embankment also resulted in deformation of the railway track, clearly visible in the LIDAR scans.

3-D LIDAR processing software was used to rotate the imagery into map view looking down from above through the roof of the portal (Figure 4c). In this view, the portal separation (36 cm) and left-lateral displacement (21 cm) from the tunnel (right) can be seen at the top and bottom of the tunnel wall. The data-hole in the center is the non-illuminated area beneath the tripod. The ability to rotate deformation imagery into any orientation to better characterize damage is one of the most powerful aspects of LIDAR technology.

Change Detection Using LIDAR Data

Damage in the aftermath of an earthquake may be ongoing and include, among other things, long term sliding, settlement, fault afterslip, geotechnical and structural collapse, and enhanced erosion or accretion of ground. One of the most useful products of terrestrial LIDAR investigation is the ability to detect changes in complex topography in the centimeter- scale with, or without DGPS control. As an example of earthquake change detection studies, we use the Parkfield-Coalinga Bridge, visible in Figure 1b, that crosses over the San Andreas Fault in the small town of Parkfield, California. On September 28, 2004, the magnitude 6.0 Parkfield earthquake resulted in minor surface rupture of the ground.. One day following the earthquake, a terrestrial LIDAR survey of the epicentral area was initiated to image ground surface and structural deformations, and establish a very detailed baseline of target positions for future surveys. Subsequently, three more LIDAR surveys were made to compare with the baseline survey from September 29. The Parkfield deformation study also allowed us to merge and

compare the surveys taken with both of the Riegl and Optech LIDAR instruments owned by the USGS. The Tripod LIDAR systems, able to resolve and map surface features a few centimeters in size, were used to target the bridge deck and piers for surface change in the months that followed the earthquake.

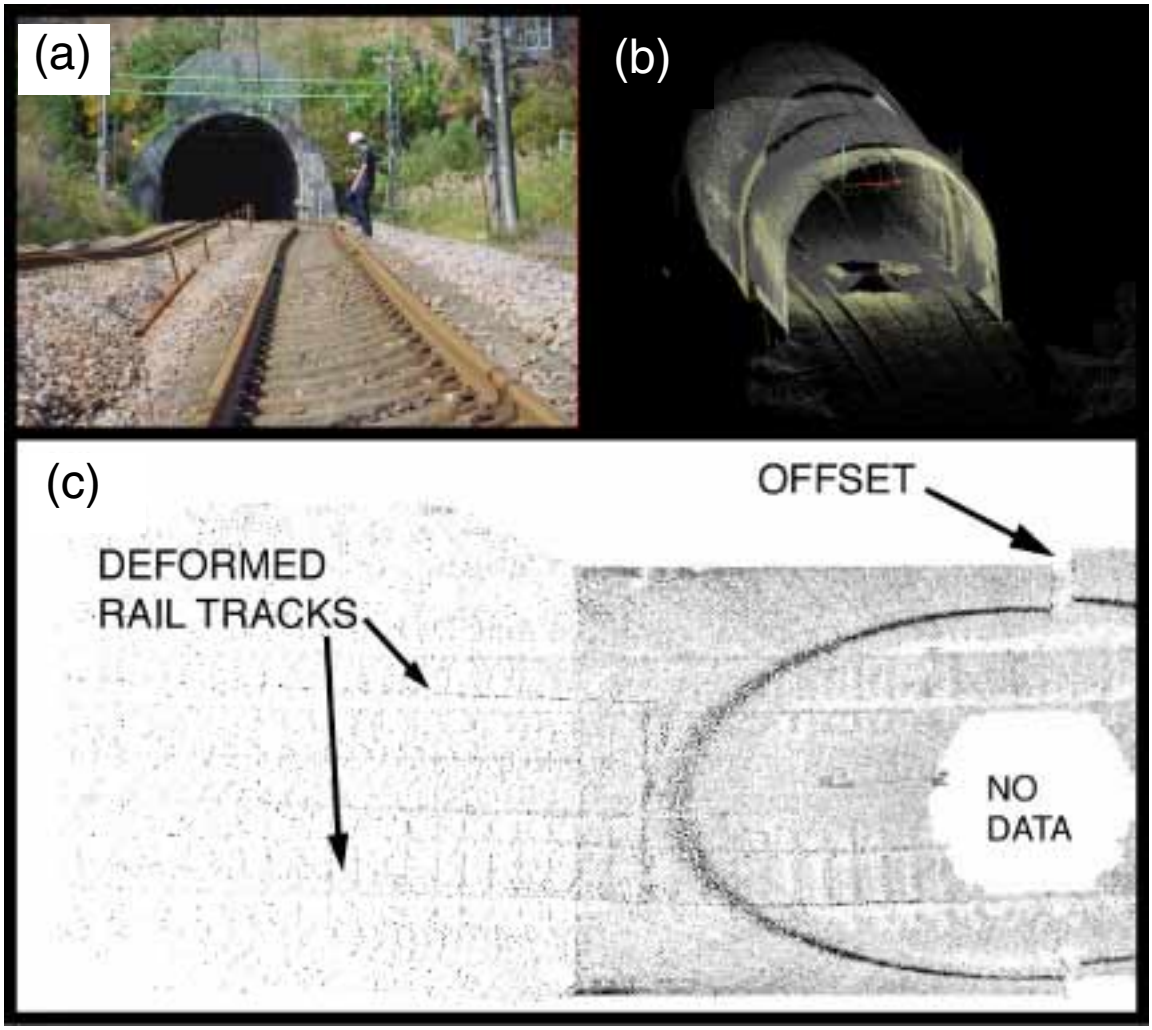

Figure 4. A photograph (a) and LIDAR image (b) of damage to a railroad portal damaged during the 2004 Niigata-Chuetsu earthquake. Lateral offset of the portal relative to the tunnel wall and distress of the rail track is precisely recorded in the LIDAR scan. A map view perspective of the LIDAR data (c) shows the portal offset to be 21 cm left lateral.

In Figure 5, the north side of the bridge is shown as well as the approximate trace of the San Andreas Fault surface rupture between the fourth and fifth piers. The white data are the individual ground targets points, and the colored data are scaled from the difference between the rendered surfaces of two sets of scans taken three months apart. The color scale, on the right indicates centimeters of lateral strain.

From the fixed vantage point of the northeast bridge abutment, it can be seen that the

first four piers of the bridge and the entire bridge deck have essentially not moved, as noted by their green-yellow color (~0 cm of change). In contrast, the fifth pier, embankment, and the road signs on the west side of the fault break are blue, indicating ground surface change of on the order of 5-6 centimeters (~2 inches) of permanent right-lateral offset of the ground. The bridge deck, decoupled from the piers, shows little change. The post-event after-slip measured on the bridge are similar to careful geodetic measurements of after-slip made by Lienkamper et al. (2004). What is remarkable about these measurements is that the two inches of afterslip deformation are small enough to not be observable to the eye except where paint marks were put on the ground immediately after the earthquake. In the LIDAR imagery, all of the fixed target on the west side of the fault rupture can be seen translated northward by approximately the same magnitude of deformation, 5-6 centimeters. That is, the LIDAR has been useful for observing small-scale tectonic changes in the ground surface, as well as large geotechnical and structural deformations.

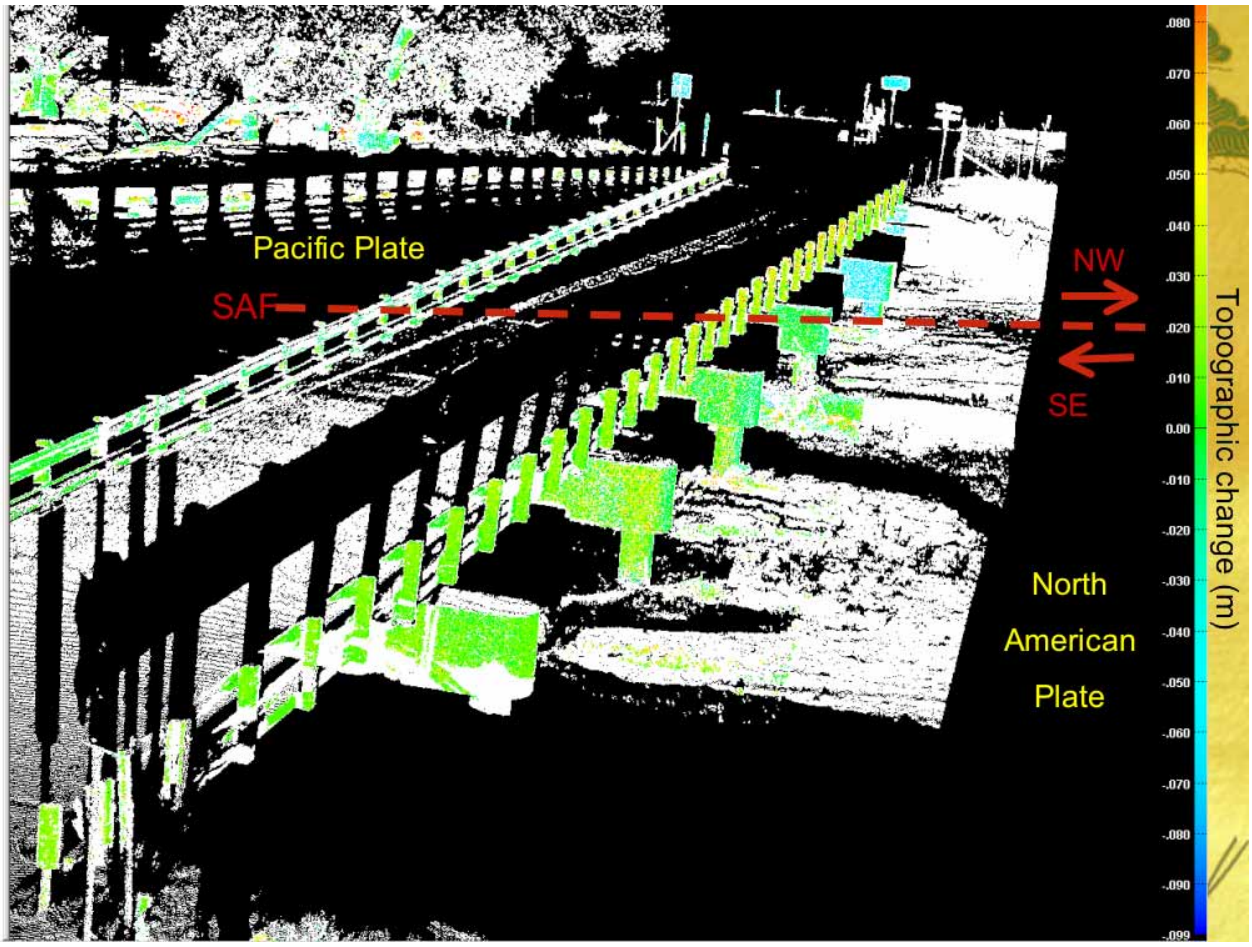

Figure 5. Change detection by differencing fused DTM surfaces at the Parkfield-Coalinga Bridge. After-slip deformations on the order of 5-6 cm on the San Andreas Fault were measured between September 29, 2004 and December 4, 2004.

Conclusions

In these studies, terrestrial tripod-mounted LIDAR systems are used to map the complex topography of earthquake damaged ground and structures, to compute deformations, and to detect and characterize changes in surfaces. There are several benefits in acquiring LIDAR data in the initial reconnaissance effort after the earthquake. First, the detailed failure morphologies of damaged ground and structures allow engineers to make measurements that are either impractical or impossible by conventional survey means. LIDAR systems can successfully resolve and map surface features that are a few centimeters in size, and precisely characterize the highly complex surfaces of large areas. LIDAR surveys can collect a huge amount of surface geometry data in a short time. This is important in rapid-response situations where clean-up and repair operations quickly destroy critical evidence. Third, digital terrain models (DTMs) allow the enlargement, enhancement, and rotation of data in order to visualize damage in orientations and scales not previously possible. This ability to visualize damage allows one to better understand failure modes. Furthermore, cross-sections and profiles can be extracted from the DTMs to further explore and understand the geometry. Where brush and trees interfere, last signal arrival data collection and post processing filtering techniques allow for the removal of vegetation, so that deformations on the bare earth can be assessed. Finally, LIDAR allows one to archive 3-D terrain models of damaged ground and structures so that the engineering community can evaluate analytical and numerical models of deformation potential against detailed field measurements. LIDAR has proven to be a useful addition to the various tools engineers and scientists bring to earthquake reconnaissance, and will likely be a standard component of future response efforts.

References

Bawden, G.W., Kayen, R., Silver, M.H., Brandt, J.T., Collins, B.D. (2004). Evaluating Tripod Lidar as an earthquake response tool, Eos Trans. AGU, 85(47), Fall Meet. Suppl., Abstract S51C-0170R.

Collins, B.D. and Sitar, N. (2004). Application of High Resolution 3D Laser Scanning to Slope Stability Studies, 39th Symposium on Engineering Geology and Geotechnical Engineering, Butte, Montana, 14 p.

Collins, B.D. and Sitar, N., (2004). Monitoring of Coastal Bluff Stability Using High Resolution 3D Laser Scanning, ASCE Geo-Frontiers Special Publication 138:- Site Characterization and Modeling, Remote Sensing in Geotechnical Engineering, E.M. Rathje, ed., ASCE, Austin, Texas, Jan 24-26, 2005.

Innovmetric. (2005). Innovmetric 3D Point Cloud Processing Software (www.innovmetric.com).

I-SiTE. (2005). 3D Laser Scanning Software. I-SiTE (www.isite3d.com).

Kayen, R., Barnhardt, W., Carkin, B., Collins, B.D., Grossman, E.E., Minasian, D., Thompson, E. (2004). Imaging the M7.9 Denali Fault Earthquake 2002 rupture at the Delta River using LIDAR, RADAR, and SASW Surface Wave Geophysics, Eos Trans. AGU,85(47), Fall Meet. Suppl., Abstract S11A-0999.

Kayen, R., Pack, R. T., Bay, J., Sugimoto, S., and Tanaka, H. (In Press). Ground-LIDAR Visualization Of Surface And Structural Deformations Of The Niigata Ken Chuetsu, 23 October 2005, Earthquake, EERI, Earthquake Spectra.

Lienkaemper, J J, Baker, B, McFarland, F S (2004). Slip in the 2004 Parkfield, California, Earthquake Measured on Alignment Arrays, AGU, 85(47), Fall Meet. Suppl., Abstract S54B-01.

Lim, M., Petley, D.N., Rosser, N.J., Allison, R.J., Long, A.J., and Pybus, D. (2005). Combined digital photogrammetry and time-of-flight laser scanning for monitoring cliff evolution. The Photogrammetric Record 20: 109-129.

Niemi, T.M., Kayen, R., Zhang, H., Dunn, C.R., Doolin, D.M. (2004). LiDAR Imagery of the San Andreas Fault Zone at the Vedanta and Olema Ridge Paleoseismic Trench Sites, Pt. Reyes, CA, Eos Trans. AGU, 85(47), Fall Meet. Suppl., Abstract G13B-0811.

Paar, G., B. Nauschnegg, and A Ullrich. (2000). Laser scanning monitoring – technical concepts, possibilities and limits. Natural Hazards Workshop, Igls Austria, 5-7 June.

Pack, R.T. (2002). Engineering geologic mapping using 3D imaging technology. 37th Annual Symposium on Engineering Geology and Geotechnical Engineering, Boise, Idaho.

RMI, 2004. LDViewer™ and LDModeler™ LIDAR Software (2005). Rappid Mapper Inc., Salt Lake City, UT. www.rappidmapper.com.

Rowens, K.A., L.D. Jones & M. Whitworth. (2003). Landslide laser scanning: a new look at an old problem. Quarterly Journal of Engineering Geology and Hydrogeology, v.36, p.155-157.

Scheikl, M., G. Poscher, and H. Grafinger. (2000). Application of the new Automatic Laser Remote Monitoring System (ALARM) for the continuous observation of the mass movement at the Eiblschrofen rockfall area, Tyrol, Austria. Natural Hazards Workshop, Igls Austria, 5-7 June.